remote sensing

MDPI

Article

Assessment of Spatio-Temporal Dynamic Vegetation Evolution and Its Driving Mechanism on the Kubuqi Desert Using Multi-Source Satellite Remote Sensing

Linjiang Nan [1,2], Mingxiang Yang [2,*], Hejia Wang [2], Ping Miao [3], Hongli Ma [3], Hao Wang [2] and Xinhua Zhang [1]

[1] The College of Water Resource and Hydropower, Sichuan University, Chengdu 610065, China; nanlinjiang@stu.scu.edu.cn (L.N.); xhzhang@scu.edu.cn (X.Z.)
[2] Department of Water Resources, China Institute of Water Resources and Hydropower Research, Beijing 100038, China; hjwang@iwhr.com (H.W.); wanghao@iwhr.com (H.W.)
[3] Inner Mongolia Erdos City River Lake Protection Center, Ordos 017000, China; m13947766004@163.com (P.M.); mhl20232023@163.com (H.M.)
* Correspondence: yangmx@iwhr.com

Abstract: Desert vegetation is undergoing complex and diverse changes due to global climate change and human activities. To effectively utilize water resources and promote ecological recovery in desert areas, it is necessary to clarify the main driving mechanisms of vegetation growth in these regions. In this study, based on MODIS and Landsat 8 remote sensing image data, the vegetation changes and driving mechanisms before and after water diversion in the Kubuqi Desert from 2001 to 2020 were quantitatively analyzed using multiple linear regression, random forest, support vector machine, and deep neural network. The results show that the average NDVI in the study area has increased from 0.08 to 0.13 over the past 20 years, and the year of NDVI mutation corresponded with the lowest precipitation, which occurred in 2010. After the water diversion, under the combined influence of human and natural factors, NDVI increased steadily without any abrupt changes, indicating that water is the main limiting factor for vegetation growth. The change of NDVI also showed obvious spatial heterogeneity, among which the improvement of the southwest irrigation area was the most significant, and the area with NDVI above 0.1 showed an expanding trend, and the maximum value exceeded 0.4. This demonstrates that moderate water diversion can reduce desert areas, expand lake areas, and promote vegetation growth, yielding positive ecological effects. The integration of multiple linear regression, support vector machines, random forests, and deep neural network methods effectively reveals the driving mechanisms of NDVI and indirectly informs future water diversion intervals. Overall, these research results can provide a reliable reference for the efficient development of water diversion projects and have high application value.

Keywords: MODIS; Landsat8; NDVI; Kubuqi Desert; ecological water diversion; spatio-temporal; driving mechanism

check for updates

Citation: Nan, L.; Yang, M.; Wang, H.; Miao, P.; Ma, H.; Wang, H.; Zhang, X. Assessment of Spatio-Temporal Dynamic Vegetation Evolution and Its Driving Mechanism on the Kubuqi Desert Using Multi-Source Satellite Remote Sensing. *Remote Sens.* **2024**, *16*, 4769. https://doi.org/10.3390/rs16244769

Academic Editor: Jose Moreno

Received: 20 October 2024
Revised: 14 December 2024
Accepted: 17 December 2024
Published: 21 December 2024

Copyright: © 2024 by the authors. Licensee MDPI, Basel, Switzerland. This article is an open access article distributed under the terms and conditions of the Creative Commons Attribution (CC BY) license (https://creativecommons.org/licenses/by/4.0/).

1. Introduction

Water diversion projects are important ecological management strategies for alleviating regional ecological water use, preventing flood disasters, and promoting vegetation recovery [1]. The response of vegetation to water is significant following ecological water transmission, and vegetation coverage on both sides of a river is improved by the water transmission project [2]. To cope with flood prevention in the Yellow River and the ecological threat to the Kubuqi Desert, Ordos explored effective ecological restoration measures. Since 2014, in the Hangjin Banner, there have been reformations and innovations with regard to sand control efforts; a new 38.5 km diversion channel and an additional 10.0 km diversion channel have been constructed within the 22 km main canal of the irrigation area on the south bank of the Yellow River. These projects divert floodwaters from the

Yellow River to the northern edge of the Kubuqi Desert. This initiative formed an ecological management area with a water surface area of approximately 25 km^2 and a wetland area of approximately 100 km^2. This helps prevent flooding of the Yellow River and the risk of dam breaks and has great significance for the construction of the ecological environment and rational utilization of water resources in the northern margin of the Kubuqi Desert. The implementation of water diversion projects requires special terrain and hydrological conditions. Currently, the main types of ecological water diversion projects in China are large-scale water diversion control projects. Relevant studies have been conducted on the impact of large-scale water diversion projects on the ecological environment [3]. However, ecological and environmental impact assessments of the small-scale water diversion project in the northern margin of the Kubuqi Desert have not been effectively conducted since the project was implemented [4].

Vegetation, an important part of global terrestrial ecosystems, plays a key role in global material cycling and energy flow [5]. Dynamic changes in vegetation are important indices that respond to the effects of human activities and climate change [6]. Desert water diversion projects are a type of human activity whose impact on the regional ecological environment can be evaluated by assessing the dynamic changes in vegetation. Only 0.10–0.35% of desert ecosystems in China are related to human activities [7]. Most previous studies have focused on the impact of natural factors on desert ecosystems, while this study considers the role of human factors, which is of great significance. Climate change directly controls the water, temperature, light, and other conditions required for vegetation growth and impacts vegetation growth [8]. With the development of remote sensing technology [9], the Normalized Difference Vegetation Index (NDVI), an important index reflecting the growth status of plants and changes in the spatial distribution of vegetation, has been widely used in related research [10]. Although there have been several studies on the mechanism of the NDVI, traditional methods are mainly used, such as mathematical statistics [11], correlation analysis [12], and trend analysis [13], which are relatively simple. These methods assume a linear relationship between vegetation changes and impact factors. However, vegetation change is affected by several factors and exhibits complex nonlinear relationships [14,15]. This study proposes a driving mechanism set that integrates linear (multiple linear regression) and nonlinear methods (random forests, support vector machines, and deep neural networks) to provide a reliable reference for local engineering practice.

The northern margin of the Kubuqi Desert is a typical arid area [16], and water diversion projects have been implemented in the study area since 2014. During the high-water level of the Yellow River flood season, part of the flood water is introduced into the lowland on the northern margin of the Kubuqi Desert following the dispatching instructions of the Yellow River Flood Control and Drought Relief Headquarters, which alleviates the pressure of flood prevention and control during the flood season. Simultaneously, part of the Yellow River was introduced into the Kubuqi Desert, which improved the ecological environment at the northern margin of the Kubuqi Desert. Promoting the management of flood resources and improving the efficiency of water resource use has become a common practice that is of great significance for ensuring the sustainable use of water resources and conforming to the national strategy of water resource development and utilization. However, because of the project operation, the mechanism of the water diversion project based on the dynamic change in regional vegetation remains unclear, necessitating alternative water diversion scales. Considering the characteristics of the water-receiving area and the time of water diversion, this study used Moderate Resolution Imaging Spectroradiometer (MODIS) NDVI data, Landsat8 data, CN05.1 meteorological data, and annual water diversion data to analyze the spatiotemporal changes in vegetation and land cover types in the northern margin of the Kubuqi Desert before and after the water diversion project and investigated the mechanisms driving vegetation change. In a word, based on multi-source remote sensing data, this paper aims to quantitatively analyze the changes in local vegetation under the background of water diversion in the Kubuqi

Desert, so as to make up for the lack of research in this area. And then, on the basis of the traditional linear mechanism, a variety of nonlinear methods are introduced to try to solve the problem that the current research methods are single and difficult to fit the actual growth of vegetation and provide a scientific basis for the reasonable planning of local ecological restoration projects, which has high application value.

2. Materials and Methods

2.1. Study Area

The Kubuqi Desert is the seventh largest desert in China, spanning the Hangjin Banner, Dalate Banner, and Zhungeer Banner of the Erdos, and is adjacent to the Yellow River on three sides in the east, west, and north. The terrain is high to the south and low to the north. The total desert area is approximately 18,600 km^2 and is located in the transition zone between arid and semi-arid climates [17]. Hangjin Banner has the largest area, accounting for approximately 50% of the county's total area. The research area is located in the Hangjin Banner section of the Kubuqi Desert, and its spatial scope was determined by field investigation and project planning (Figure 1).

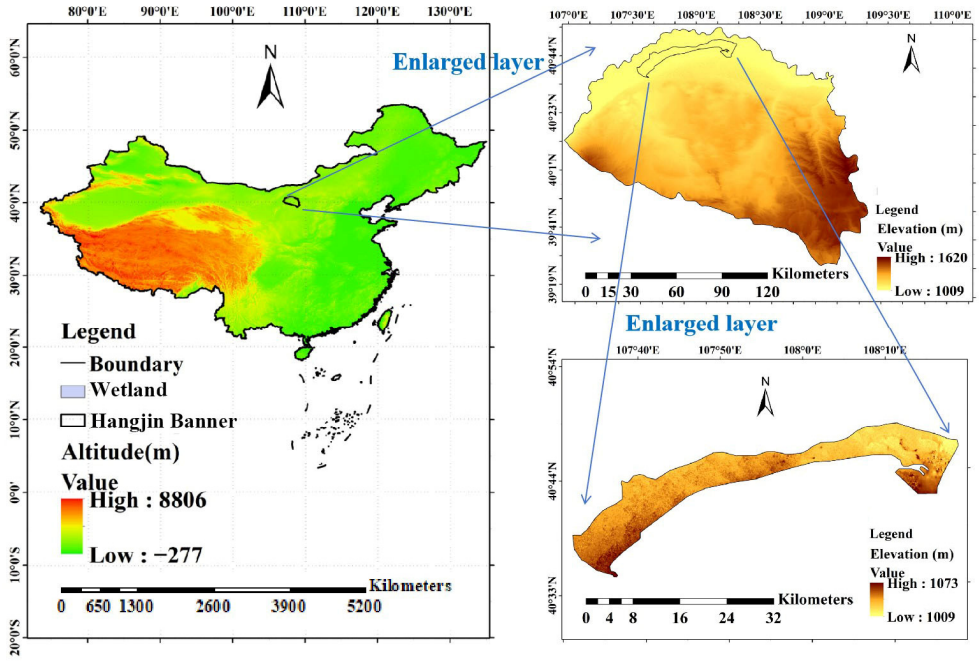

Figure 1. Geographical location of the study area.

The Kubuqi Desert is a typical desert landform dominated by mobile dunes, which account for approximately 61% of the total desert area. The main dunes were dune chains, lattice dunes, and compound dunes. Semi-fixed dunes account for 13% of the total desert area, while the fixed dunes 26%, mostly distributed on the desert edge. The study area was mostly distributed in fixed dunes.

The annual precipitation in the study area is relatively small, only 250–360 mm, concentrated in June to August, and shows high spatial heterogeneity, specifically decreasing from southeast to northwest. In addition to low rainfall, the local drought is also affected by high evaporation and wind speed.

Overall, the study area is dry year-round with minimal amounts of rain and substantial evaporation, abundant sunshine, long and cold winters, and mild and short summers. Whether water diversion can effectively reduce sandy areas and improve local ecological conditions remains to be determined.

2.2. Data

2.2.1. Moderate Resolution Imaging Spectroradiometer Data

The MODIS NDVI product MOD13A3 was provided by the National Oceanic and Atmospheric Administration and has a spatial resolution of 1 km and a temporal resolution of 1 month [18]. The MODIS NDVI dataset has the advantages of continuous-time and high spatial resolution and is widely used in vegetation growth monitoring [19].

In this study, MODIS NDVI data from 2001 to 2020 were selected as the basic data sources according to the research requirements. The imaging effect was good, and the cloud cover was maintained below 10%. Data sources and preprocessing were based on the Google Earth Engine platform.

2.2.2. Landsat Data

This study used Landsat8 data with a spatial resolution of 30 m from the United States Geological Survey (https://earthexplorer.usgs.gov/, URL (accessed on 17 September 2023)), widely employed in the spatial distribution of NDVI and land use analysis [20]. Since the Landsat8 data source commenced in 2013, this study selected data from 2013 to 2020 for NDVI spatial feature analysis. In addition, satellite images of the annual growing season (June–September) before the water diversion (2013), the minimum water diversion year (2014), and the maximum water diversion year (2019) were selected to analyze land use change.

The cloud cover of the Landsat8 satellite data were maintained at <5%. Since the data source was geometrically corrected, only radiometric calibration and atmospheric corrections were required after acquisition.

2.2.3. Meteorological Data

In this study, daily CN05.1 data, including precipitation, average temperature, maximum temperature, minimum temperature, relative humidity, wind speed, and sunshine duration, were obtained from 2001 to 2020 from the ecological management area of the Kubuqi Desert. The data were obtained from the China Meteorological Data Network (https://data.cma.cn/, URL (accessed on 20 November 2023)).

2.3. Methods

In this paper, Sen slope estimation and the pettitt mutation test are used to analyze the change characteristics of NDVI. When analyzing the driving mechanism of NDVI, a variety of factors are considered. Not only is the conventional multiple linear regression adopted, but also a variety of nonlinear methods are introduced, including random forest (RF), support vector machine (SVM), and deep neural network, which have the advantage of being more suitable for the actual situation of vegetation. In addition, the SVM supervised classification method was used to invert land use types, and overall accuracy (OA) and the kappa coefficient were combined to evaluate classification accuracy.

The flowchart of the method adopted in this paper is shown in Figure 2, and the specific principle of the method is shown in each section.

2.3.1. NDVI Calculation Method

The NDVI is a standardized index used to produce images showing the amount of vegetation (relative biomass). This index compares the characteristics of the two bands in the multispectral raster dataset: the pigment absorption rate of chlorophyll in the red band and the high reflectance of plants in the near-infrared band. Since the reflectance values of the red and infrared bands differ, the spectral reflectance of solar radiation can be used to monitor the density and intensity of green vegetation growth. Typically, green leaves reflect more in the near-infrared wavelength range than in the visible wavelength range. When the leaves are dehydrated, sick, or dead, they become more yellow; thus, reflection

in the near-infrared range is significantly reduced. Therefore, the value range of NDVI is [−1, 1]. The calculation formula is as follows [21]:

$$\mathrm{NDVI} = \frac{\rho_{NIR} - \rho_{RED}}{\rho_{NIR} + \rho_{RED}} \quad (1)$$

where ρ_{NIR} represents the reflectivity of the near-infrared band and ρ_{RED} represents the reflectivity of the red band.

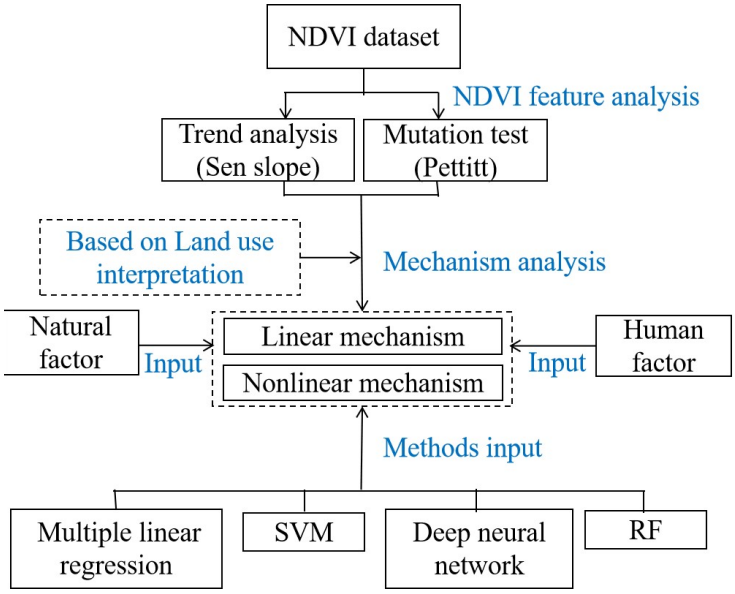

Figure 2. Flowchart of the methods.

2.3.2. Trend Analysis Method

In this study, the Sen slope method, which is commonly used to calculate the trend of time-series data, was used to calculate the annual change trend of NDVI in the study area using the following formula [22]:

$$\beta = \mathrm{Median}\left(\frac{X_j - X_i}{j - i}\right) \quad \forall j > i \quad (2)$$

where X_j, X_i are the NDVI values of years j and i, respectively, and the median is a function of taking the median value.

2.3.3. Mutation Test

The Pettitt mutation test is a non-parametric mutation detection method that is simple to calculate, less affected by outliers, and widely used for mutation analysis of hydrometeorological elements [23].

Pettitt defined the statistic $K_t = \max_{1 \le t \le n} |U_t|$ to obtain the most significant possible mutation point, and the statistic $P = 2\exp\left[\frac{-6K_t^2}{n^3+n^2}\right]$ was used to determine whether the mutation point met the given significance level. $p < 0.05$ indicates a statistically significant mutation point, where U_t is the statistical variable of the sample time series and n is the number of sample series.

2.3.4. Multiple Linear Regression

A linear regression relationship exists between multiple (more than two) elements, referred to as a multiple linear regression [24]. If the dependent variable y is subject to k

explanatory variables X_1, X_2, …, X_k, then the structure of the multiple regression model is as follows [25]:

$$y = \beta_0 + \beta_1 X_1 + \beta_2 X_2 + \cdots + \beta_n X_n \quad (3)$$

2.3.5. Random Forest

Random Forest (RF) is an integrated algorithm created by introducing bootstrap aggregation based on a classification regression tree (CART) [26]. Given a training set $X = X_1, X_2, \ldots, X_n$ and response variable Y (X is the driving factor; Y is NDVI), Bootstrap is repeated B times ($b = 1, 2, \cdots, B$) to put back random sampling to construct the sample set [X_b, Y]. The tree fitting f_b was then performed, and the training data were projected into the random subspace before fitting to increase the variation between different carts. To avoid overfitting, the final prediction of the RF was defined as the average output per CART, and the general function is:

$$f_i^p = \sum_{k=1}^{l} f_k(X_i) = f_i^{p-1} + f_i(X_i) \quad (4)$$

where f_i^p is the prediction result generated by CART for i input sample X_i in the iteration.

2.3.6. Support Vector Machine

Support vector machine (SVM) has unique advantages in solving small-sample, nonlinear, and high-dimensional pattern recognition problems. The principle of structural risk minimization replaces the empirical risk minimization principle adopted by traditional learning machines and can effectively prevent overfitting. Therefore, it is considered the best theory for classification and regression of small sample sizes [27].

The optimal hyperplane decision function of a linear support vector machine is:

$$M(x) = Sgn((w^* \cdot x) + b^*) = Sgn\left(\sum_{S.V.} a_i^* y_i (x \cdot x_i) + b^*\right) \quad (5)$$

where $Sgn()$ is a symbolic function; a_i^*, b^* are the parameters for determining the optimal partition hyperplane; x, $x_i \in R^N$ is an n–dimensional vector, x is a point on the hyperplane, x_i is the sample data set, $(x \cdot x_i)$ is the dot product of two vectors, and $y_i \in \{1, 2, \ldots, k\}$ is divided into k classes.

For linear indivisibility, the sample space was mapped into a high-dimensional feature space by nonlinear mapping φ. Therefore, the highly nonlinear problems in the sample space can be realized in the high-dimensional feature space using the linear classification method. Since a linear classification method is adopted in the feature space, the optimal hyperplane decision function in the feature space is

$$M(x) = Sgn((w^* \cdot \varphi(x) + b^*) = Sgn\left(\sum_{S.V.} a_i^* y_i (\varphi(x) \cdot \varphi(x_i)) + b^*\right) \quad (6)$$

According to Mercer's theorem, the optimal hyperplane decision function of a nonlinear support vector machine can be obtained as

$$M(x) = Sgn((w^* \cdot \varphi(x) + b^*) = Sgn\left(\sum_{S.V.} a_i^* y_i K(x, x_i) + b^*\right) \quad (7)$$

where $K(x, x_i) = (j(x) \cdot j(x_i)$ is Mercer kernel. Mercer kernel function calculation replaces the point product calculation, and the display expression of nonlinear mapping is not required in the whole solution process; therefore, the increase in the calculation amount was negligible compared with the linear method. However, the linear division of feature space corresponds to the highly nonlinear division of the original sample space.

2.3.7. Deep Neural Network

Deep neural networks are a type of artificial neural network with multiple hidden layers based on perceptrons [28]. The neural network layer inside a deep neural network

can be divided into three categories: input, hidden, and output layers. The first layer is the input layer, the last layer is the output layer, and the middle layer is the hidden layer. The data enters the network through the input layer, which is determined by the dimensions of the actual input data, flows backward through each layer, and finally reaches the output layer. There are n hidden layers in the middle of the network; each layer contains several neurons, and the layers are fully connected. For example, any neuron in layer i must be connected with any neuron in layer $i + 1$. For the local model between each neuron, the calculation includes two parts: linear transformation and an activation function. This is used to add nonlinear factors, solving problems that linear models cannot. Activation functions were used between different network layers to induce the response of neurons to stimulation. By selecting different activation functions and dynamically blocking the connections between the neurons in the front and back layers, the model can better learn the nonlinear features of the data and avoid over-fitting.

2.3.8. Land Use Interpretation

In this study, after radiometric calibration and atmospheric correction of Landsat8 images, the SVM supervised classification method combined with visual interpretation techniques was adopted for land-use classification. Some small image spots were produced in the preliminary classification results, affecting the overall classification. To improve accuracy, post-processing was conducted by combining the intelligent classification of majority/minority with manual visual interpretation.

Majority/Minority Analysis uses a method similar to that used for convolution filtering to classify false pixels in a larger class into this class and to define the size of the transform kernel [29].

After land classification, overall accuracy (OA) and kappa coefficient are used to evaluate the accuracy of the land-use inversion results with the verification samples.

Overall Accuracy (OA)

The overall classification accuracy represents the probability that any sample is correctly classified (the classification result is the same as the actual land class) and is widely used in the accuracy assessment of land-use classification [30]. The size of P_0 is determined by the quotient of the number of correctly classified samples and the total number of samples and is calculated as follows:

$$\mathrm{OA} = \sum_{i=1}^{n} \frac{P_{ii}}{P} \tag{8}$$

where OA represents the overall classification accuracy, n represents the number of sample categories, P_{ii} represents the number of correctly classified Class i samples, and p represents the total number of samples.

Kappa Coefficient

The kappa coefficient is a commonly used precision evaluation index used to quantitatively evaluate whether a pixel is effectively sampled to the correct LUCC type [31]. In this paper, the kappa coefficient is used as an auxiliary index to verify the evaluation results of OA, and its calculation formula is as follows:

$$\mathrm{Kappa} = \frac{N\sum_{i=1}^{r} X_{ii} - \sum_{i=1}^{r} X_{i+}X_{+i}}{N^2 - \sum_{i=1}^{r} X_{i+}X_{+i}} \tag{9}$$

where r is the number of columns in the confusion matrix, X_{ii} is row I, the number of samples in column i is the number of samples that are correctly classified, X_{i+} is the number of samples in row I, X_{+i} is the number of samples in column i, and N is the total number of verification samples.

3. Results

3.1. Meteorological Element Analysis

Daily scale CN05 data of the ecological management area of Kubuqi Desert from 2001 to 2020 were used as meteorological factors affecting NDVI, including annual precipitation (Pre), annual sunshine duration (SSD), average temperature (Tem), wind speed (Wind), maximum temperature (Tem-max), and minimum temperature (Tem-min). Their interannual variation trends are shown in Figure 2.

In Figure 2, annual precipitation, average temperature, maximum temperature, and minimum temperature in the study area show an increasing trend over the past 20 years, consistent with previous findings [32]. Relative humidity declined as sunshine duration, wind speed, and temperature increased, enhancing local evaporation.

3.2. NDVI Trend Analysis

In this study, the Sen slope estimation method was used to analyze the MODIS NDVI trend in the ecological management area of the Kubuqi Desert from 2001 to 2020. The results are shown in Figure 3.

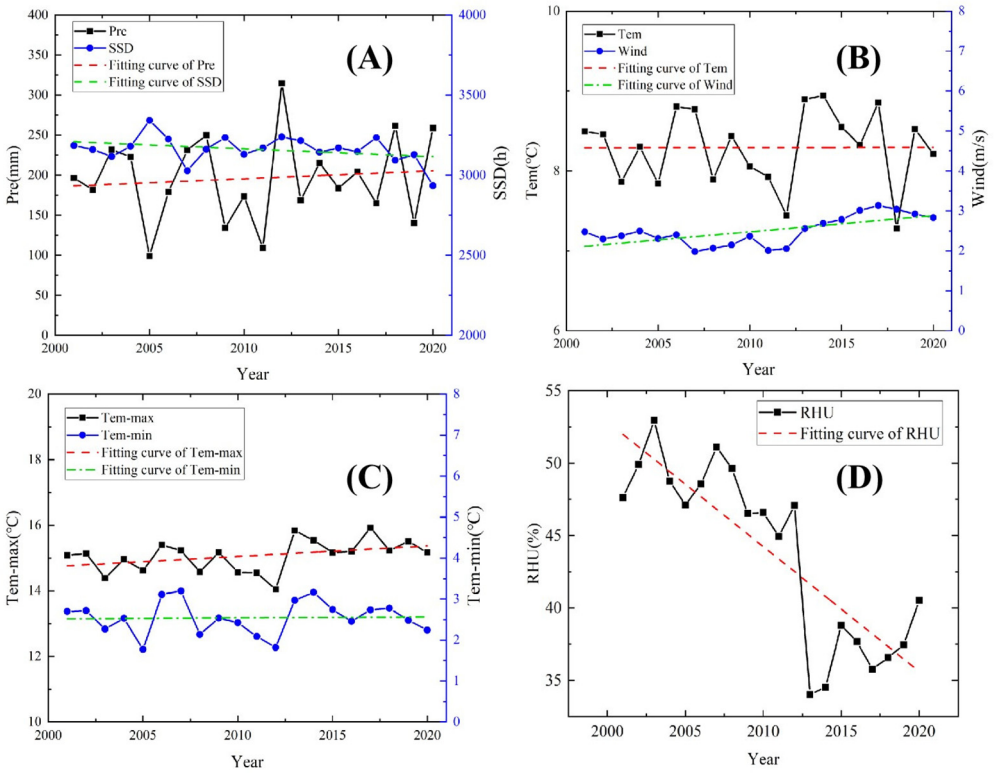

Figure 3. Interannual variation trend of meteorological elements in the ecological management area from 2001 to 2020. ((**A**) indicates the variation trend of Pre and SSD; (**B**) indicates the variation trend of Tem and Wind; (**C**) indicates the variation trend of Tem-max and Tem-min; (**D**) indicates the variation trend of RHU).

The slope calculated using Sen's method was 0.0031; that is, the NDVI in the study area from 2001 to 2020 showed an upward trend, which was consistent with previous results [33]. Overall, the NDVI in the study area has increased from 0.08 to 0.13 over the past 20 years, which is related to improving local hydrothermal conditions. The increase in temperature and sunshine duration provides more heat energy for vegetation growth, which is conducive to plant photosynthesis. However, the annual precipitation shows an increasing trend, providing better water conditions for vegetation [34].

3.3. NDVI Mutation Test

The interannual variation characteristics of the NDVI in the study area showed fluctuating changes in the series. To further reveal the change rule of the NDVI, this study adopted the Pettitt method to conduct mutation tests. The results are shown in Figure 4.

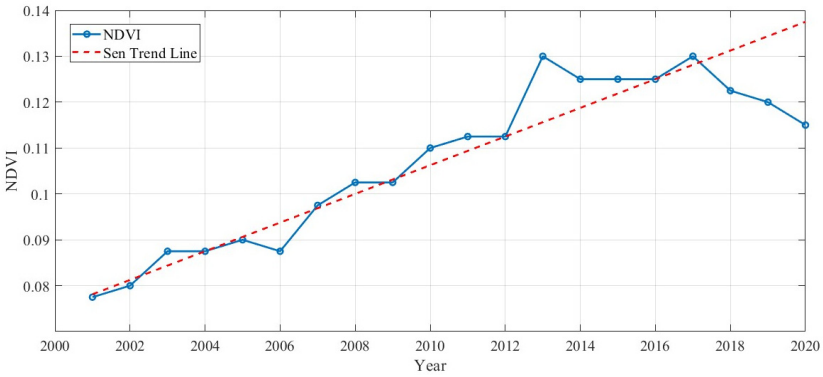

Figure 4. NDVI time series based on the Sen trend line.

The mutation of NDVI occurred in 2010 when no water was diverted, and annual precipitation was the lowest in recent years, which directly affected the growth of local vegetation and led to the mutation of NDVI. The main limiting factor of vegetation growth in the Kubuqi Desert is water, and the change in precipitation will have a substantial impact on vegetation, consistent with previous findings [35]. In addition, no mutation in vegetation growth status was caused by water diversion, indicating that NDVI in desert environments is influenced by natural and human factors [36] and that its driving mechanism is complex and needs further exploration.

3.4. Spatial Variation Characteristics of NDVI

Since the introduction of water, NDVI has shown a marked improvement across the area, with the most significant changes occurring in the southwest (Figure 5). This is because the irrigation area is located in the southwest of the study area. As irrigation progresses, the area with NDVI above 0.1 expands, with a maximum value above 0.4, indicating improved vegetation coverage. Furthermore, according to the research of Dai et al. [37], the vegetation in this area is primarily desert grassland. This is because herbaceous plants are highly adaptable to the environment and can efficiently utilize water [38]. Additionally, their shorter growth cycle allows them to quickly cover the ground and form a dense vegetation layer. The herbaceous plants in the desert, which thrive first after water introduction, are designed to rapidly form vegetation cover to prevent water evaporation and soil erosion, thereby creating favorable conditions for subsequent vegetation recovery and ecosystem reconstruction.

In the central region of the study area, there are only small patches of NDVI above 0.1, scattered sparsely (Figure 6). This is because the area is currently outside the influence of the irrigation zone and does not receive an effective water supply, hindering local vegetation recovery.

In the northeastern part of the study area, a large area with NDVI above 0.1 is present due to its proximity to the Yellow River wetland and irrigation area. Groundwater is easily replenished in this region, maintaining a certain level of vegetation cover.

In summary, the implementation of the irrigation project has brought notable ecological effects to the desert management area, with the most significant improvements observed in the southwest irrigation area.

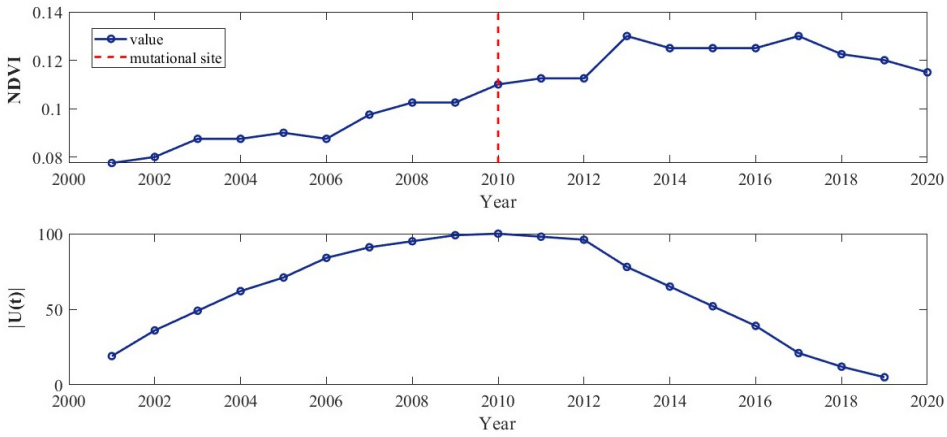

Figure 5. Results of the Pettitt mutation test.

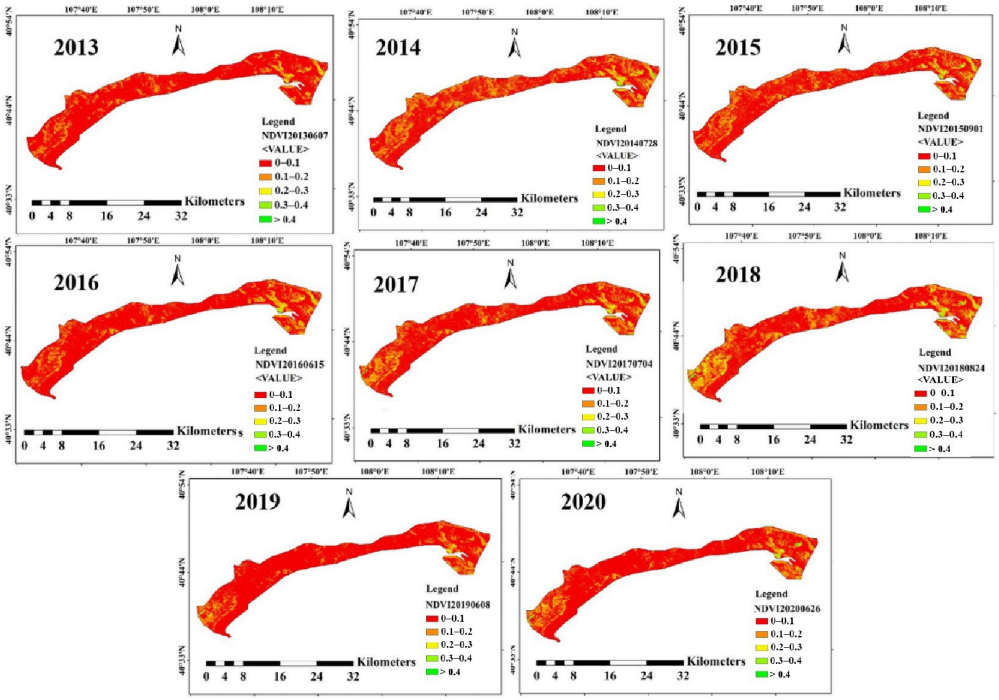

Figure 6. NDVI spatial distribution before and after water diversion in the ecological management area.

4. Discussion

The changes in NDVI within the ecological management area are primarily influenced by both human and natural factors. Human factors mainly involve land use changes resulting from water diversion, while the natural factors primarily include various meteorological elements that together impact vegetation growth conditions [39].

4.1. Land Use Change Analysis

To more intuitively represent the impact of water diversion on vegetation, this study used Landsat8 satellite data to invert land use changes before water diversion (2013), with the smallest amount of water diversion in 2014 and the largest amount of water diversion in 2019.

The true color is close to the actual color of the ground object, and the false color can highlight the color of the vegetation in the study area as red, which is easy to classify. Therefore, in the inversion process, the training samples were selected based on the true and false color images of the combination of 4, 3, 2 and 5, 4, 3 bands, respectively, so as to

improve the accuracy of land use classification. The display effect of true and false color composition and the spectral attribute among lakes, grassland, and desert are shown in Figure 7.

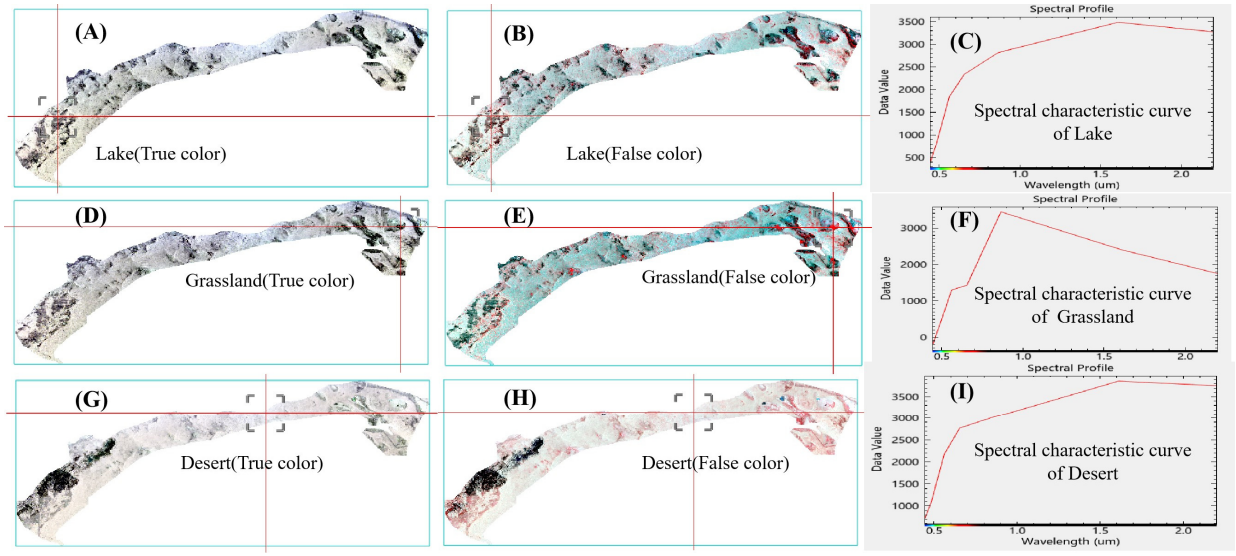

Figure 7. Image display and spectral attribute ((**A**–**C**) represent true and false color composition and the spectral attribute of the lake in 2013, respectively; (**D**–**F**) are for Grassland in 2014, and (**G**–**I**) are for desert in 2019).

This study considered 2013 as the reference year and generated land-use spatial change maps from 2013–2014 and 2013–2019, as shown in Figure 8.

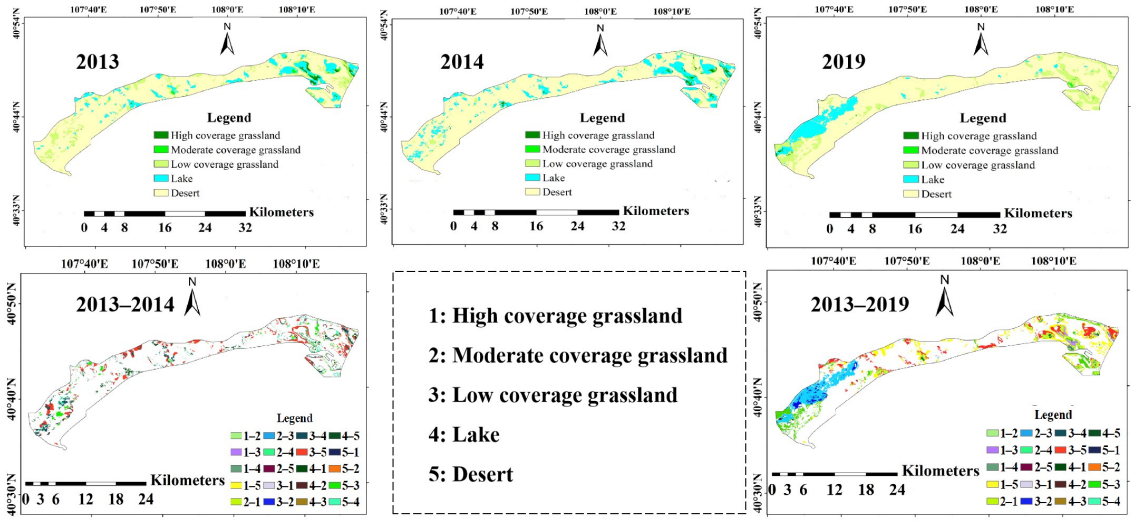

Figure 8. Spatial change map of land use in the ecological management area.

Table 1 shows the evaluation results of classification accuracy, which can be seen that the overall accuracy is >96%, and the Kappa coefficients were >0.8, indicating a good inversion effect [40].

Table 1. Results of land use classification accuracy evaluation.

Year	OA (%)	Kappa
2013	96.50	0.87
2014	96.99	0.89
2019	97.50	0.89

The results showed that the change in sandy land was not significant during the initial stage of water diversion in 2014. In the southwestern part of the study area, a small area of sandy land was transformed into lakes and grasslands, the central part was mainly sandy land, and the northeastern part was scattered with grasslands and lakes. In 2019, a large area in the southwest of the study area was transformed into a lake; the grassland area was significantly expanded and mainly distributed around the lake. The central area was sandy. The northeast was scattered with small grasslands and lake areas.

Overall, the lake area in the southwest of the study area expanded, with a large range of grasslands, because water diversion directly occurred in this area. Additionally, the ecological effect of continuous water diversion can be intuitively displayed. The water diversion from the southwest indirectly increased the local groundwater, thus providing conditions for vegetation growth, whereas the lakes formed by the diversion of water can regulate the local water cycle and increase precipitation, conducive to vegetation growth. Few lakes were in the northeast whose areas were constantly changing because the northeast was near the Yellow River, and groundwater could be effectively replenished. However, the areas of local lakes and grasslands varied significantly yearly, which is related to the status of the Yellow River inflow, local precipitation, temperature, and evapotranspiration. Continuous water diversion reduced the sandy area and has a more obvious ecological effect.

To quantitatively analyze the impact of continuous water diversion on the local ecological status, the land use transfer matrix [41] was adopted in this study to conduct an in-depth analysis of the land change status in the ecological management areas from 2013 to 2014 and 2013 to 2019 (Table 2). This enabled the transformation of different land use types caused by water diversion to be comprehensively and intuitively reflected [42] and showed the dynamic change of vegetation.

Table 2. Land use transfer matrix in the ecological management area.

Land Cover Area (Km^2)		2013				
		A	B	C	D	E
2014	A	1.84	0.76	0.75	1.24	0.18
	B	0.71	0.32	0.35	0.15	0.12
	C	0.05	0.08	5.04	0.12	5.98
	D	1.90	1.34	12.53	34.58	5.61
	E	0.13	0.11	24.81	5.14	283.16
2019	A	0	0	0.16	0.22	0.19
	B	0.66	0.08	0.04	0.28	0.01
	C	3.35	1.88	13.48	16.75	19.26
	D	0.07	0.03	5.06	4.58	31.11
	E	0.56	0.63	24.79	19.38	244.64

A represents high coverage grassland; B represents moderate coverage grassland; C represents low coverage grassland; D represents lake; E represents desert.

As can be seen from the land use type transfer matrix from 2013 to 2014, 11.89 km^2 (4.03%) of sandy land in the region was transformed into grassland (2.1%) and lake (1.9%). Although there was a certain ecological effect, it was not obvious because the transformation was in the early stages of water transfer in 2014. The total water transfer was low (2,831,600 m^3); therefore, it was difficult to show significant changes in a short period. The land-use transfer matrix from 2013 to 2019 showed that 6.59% of sandy land was converted

to grassland and 10.54% was converted to lakes. Among them, the sandy land was more easily transformed into low-cover grassland (19.26 km^2), while the ability to transform into medium and high-cover grassland (0.2 km^2) was lower. Certain low-coverage grasslands were transformed into medium- and high-coverage grasslands, whereas moderate-coverage grasslands were transformed into high-coverage grasslands. However, the grassland coverage in small areas was reduced because of the desert climate, sparse rainfall, high summer temperatures, cold winter temperatures, and strong winds. These harsh environments pose significant challenges to grassland stability. Maintaining high levels of grassland coverage in certain areas is difficult.

Overall, ecological water diversion reduced the range of sandy land, expanded the lake area in the region, and played a significant role in promoting the growth of local vegetation. The influence of desert water diversion on grasslands can be considered from several perspectives. Desert areas typically lack water resources, resulting in sparse vegetation and desertification. By introducing water sources, the ecological environment of desert areas can be improved to a certain extent, and vegetation growth and recovery can be promoted. This will help to form more grasslands, increase vegetation coverage, slow down soil erosion, and prevent desert expansion, thereby protecting land resources and maintaining ecological balance. Second, the influence of desert water diversion on grasslands involves changes in soil quality and moisture. Since the soil in desert areas is usually dry and barren, lacking water and nutrients and limiting the growth and development of grassland, the introduction of water resources can improve the soil water status and fertility and provide more favorable conditions for the growth of grassland. Continuous water diversion also has a certain negative impact on local vegetation because the water diversion changes the type of land use and expands the area of the lake, thus inundating some vegetation or affecting its living space; the excessively humid zone adjacent to the lake will inhibit vegetation growth [43].

Thus, vegetation change is affected by various factors and has a certain complexity [44], and it is necessary to reveal its internal driving mechanism to provide a reference for the efficient development of water diversion projects.

4.2. NDVI Driving Mechanism Analysis

In recent years, owing to the complexity of regional climate change and the diversity of anthropogenic interference, elucidating the mechanism underlying NDVI influence has attracted research attention [45]. Although researchers have analyzed the mechanism underlying the influence of vegetation change, most have adopted the traditional linear method. However, vegetation changes are often affected by many factors, resulting in complex nonlinear relationships. The nonlinear relationship depends on the interactions between various factors; therefore, it is difficult to quantify the driving force of each factor [46].

The spatial change characteristics of the NDVI show that the water intake area southwest of the ecological management area has significant vegetation changes. To analyze the NDVI impact mechanism more accurately, this study extracted the NDVI average value from 2001 to 2020 for the Bayin Wenduer Wetland, the main impact area in the southwest, and proposed a set of impact mechanisms, including linear and nonlinear mechanisms. This is of great significance for the efficient implementation of water diversion projects in the future.

4.2.1. Linear Mechanism

In this study, the maximum NDVI value and nine natural and anthropogenic factors (annual precipitation, average air temperature, maximum air temperature, minimum air temperature, wind speed, relative humidity, annual sunshine duration, annual water diversion, and cumulative water diversion) of the Bayin Wenduer Wetland in the southwest of the ecological management area were simulated using multiple linear fitting. First, the six main driving factors were selected using multicollinearity theory. By considering

2001–2016 as the training set and 2017–2020 as the verification set, the model was driven, and the following relationship was obtained:

$$\begin{aligned} \text{NDVI} = 0.01 + 0.28 \times \text{Pre} - 0.09 \times \text{Tem} - 0.05 \times \text{Win} - 1.02 \times \text{RHU} + 0.07 \\ \times \text{SSD} - 0.02 \times \text{Div} + \varepsilon \end{aligned} \quad (10)$$

Here, Pre is the annual precipitation, Tem is the average temperature, Win is the wind speed, RHU is relative humidity, SSD is the annual sunshine duration, Div is the annual water diversion, and ε is the error.

The MSE, RMSE, and correlation coefficient of the above multiple linear regression equation are 0.09, 0.30, and 0.87, respectively, indicating that the error is low, the correlation is high, and the model fit is good. In the equation, NDVI is positively correlated with annual precipitation and annual sunshine duration, which is consistent with the findings of Liu et al. [47]. There was a negative correlation with other factors. Among them, NDVI shows a higher significance level with annual water diversion, wind speed, and sunshine hours, with correlation coefficients of 0.92, 0.81, and 0.72, respectively.

Water diversion directly changes the land use type, transforming sandy land and grassland into lakes and inundating local vegetation. As a result, when water diversion exceeds a certain threshold, the growth rate of NDVI decreases. Thus, water diversion has two effects on the growth of local vegetation: on one hand, it can supplement the water supply, improve sandy conditions, and promote terrestrial vegetation growth. On the other hand, as water diversion increases, the expanding lake area submerges vegetation. Additionally, prolonged water retention can lead to local soil salinization, which damages the vegetation's growth environment.

Although water and heat conditions are limiting factors for vegetation growth, the Kubuqi Desert receives relatively little annual precipitation, has low air humidity, and faces harsh natural conditions, making it easier for drought-tolerant herbs to grow, thereby weakening the influence of precipitation, temperature, and humidity. Moreover, local wind speeds have increased over the past 20 years, accelerating water evaporation and promoting soil desertification. This reduces the soil's organic matter content, leading to poor soil fertility, which is unsuitable for vegetation growth [48] and significantly hinders the growth of vegetation. Furthermore, in desert areas, the lack of water resources means that higher temperatures increase vegetation transpiration, further limiting growth. Sufficient sunshine, however, provides abundant energy for vegetation growth near water-receiving areas and accelerates photosynthesis, resulting in a strong positive correlation.

4.2.2. Nonlinear Mechanism

In this study, a support vector machine, random forest, and deep neural network were used to analyze the mechanism underlying the influence of NDVI in the Bayin Wenduer Wetland from 2001 to 2020 based on the main impact factors determined using the multiple linear regression method. Data from 2001 to 2016 were used as the training set, while data from 2017 to 2020 were used as the verification set to drive the three types of models. The simulation results are listed in Table 3.

Table 3. Simulation effect of nonlinear mechanism.

Method Class	RMSE	MSE	R^2
SVM	0.28	0.08	0.32
Random forest	0.29	0.08	0.88
Deep neural network	0.19	0.04	0.96

The results show that the error of the three nonlinear methods is low and suitable for constructing the mechanism underlying the influence of NDVI in the Bayin Wenduer Wetland. The deep neural network method has the best simulation effect and can provide more reliable information, followed by random forest technology. The random forest model

had a higher fault tolerance rate for noisy data and performed better in robustness and operational efficiency. Li et al. [49] used various models to invert the NDVI and reported that random forest had the best effect. Jin et al. [50] used machine learning to invert the above-ground biomass of the grasslands on the Qinghai-Tibet Plateau, and the results showed that the random forest model was superior to the other 23 models. The advantages of deep neural network methods include high prediction accuracy, strong adaptability, wide coverage, and strong learning abilities, which have been widely applied in domestic and foreign research. Huang et al. [51] reported that the prediction accuracy of deep neural networks was higher than that of traditional methods, reaching 98.2%. Zhang et al. [52] showed that the simulation effect of the deep neural network method was better than that of the classical traditional method, and its stability was stronger. Therefore, this study selected random forest and Deep neural network methods to perform the next step of the prediction work. The target level of vegetation growth in the study area (i.e., NDVI) and natural factors under future climate conditions (annual precipitation, average annual temperature, wind speed, relative humidity, and annual sunshine duration under future climate models) can be input into various models to obtain future annual water diversion. Subsequently, the upper and lower limits of water diversion were obtained according to the simulation results of the random forest and deep neural network to provide a reliable reference for the efficient development of water diversion projects.

In summary, support vector machine (SVM), random forest, and deep neural network model have been widely used and proved to have high accuracy. Therefore, this paper combines the advantages of the above three methods to analyze the driving mechanism of NDVI more reasonably and accurately.

4.3. Effects on Other Species

The Kubuqi Desert ecosystem itself is relatively fragile, with sparse vegetation and relatively low biodiversity due to its lack of water. Diversion projects change the distribution of water resources in the desert, which will not only affect the growth of vegetation but also affect other organisms.

Ecological water diversion has both positive and negative effects on local animals. On the one hand, diverting water will improve the habitat of animals. Increased vegetation provides more habitat and food sources for insects, birds, small mammals, etc. At the same time, water diversion may attract a greater variety of animals, including waterfowl and other water-dependent organisms, thereby increasing species diversity. On the other hand, it will cause a series of problems such as habitat competition. Water sources such as lakes in deserts can attract large concentrations of organisms, which can lead to increased competition, threaten original animal populations, and even imbalance predator-prey relationships.

In addition, the water diversion project can also have an impact on local microorganisms and soil. On the positive side, water diversion enhances soil activity. Increased moisture promotes soil microbial activity and helps nutrient circulation. On the negative side, the continuous diversion of water will also cause an increase in pathogenic microorganisms. High humidity environments may allow certain harmful microorganisms to multiply, adversely affecting the health of plants and animals.

4.4. Policy Implications

All kinds of NDVI driving mechanism models proposed in this paper have good simulation effects, so they can reverse calculate the range of water diversion based on future climate scenarios and the expected growth of local vegetation, so as to provide reliable data support for the efficient operation of the project and have important reference value for local water resources management and sustainable utilization [53].

4.5. Limitations in Terms of Data and Methods

Although this study considered many natural factors affecting vegetation growth, due to the actual situation of data acquisition, the influence of evaporation, slope, slope direction, elevation, and other factors was not analyzed. Secondly, the water diversion data are on an annual scale, which can be refined to a monthly or daily scale according to the actual engineering situation in subsequent studies, so as to better reflect the driving mechanism of vegetation change.

In addition, various methods are used to analyze the driving mechanism of various factors on a time scale, but there is a lack of spatial analysis. Therefore, the contribution degree of natural and human factors to NDVI in space can be discussed in the subsequent research, so as to quantitatively analyze the main driving factors of vegetation and the influence range of the water receiving area after water diversion, in order to provide references for the efficient operation of water diversion projects.

4.6. Perspectives for Future Research

First of all, the accuracy of remote sensing data sources is an important basis for research, so it is necessary to adopt appropriate methods to fully integrate the current mainstream remote sensing data sources such as Modis, Landsat, and sentinel. Secondly, the study area is located in a desert uninhabited region, and there are no agricultural activities such as grazing and planting during the study period. Human activities only need to consider the impact brought by ecological water diversion projects, but the resolution of water diversion data should be improved to the scale of month or day. Finally, it is necessary to strengthen the analysis of the vegetation driving mechanism on the spatial scale according to the actual situation and get the range of optimal water diversion under the ideal growth condition of vegetation.

5. Conclusions

This study used multi-source satellite remote sensing data to quantitatively analyze vegetation change and the mechanisms underlying its influence in the ecological management area of the Kubuqi Desert before and after water diversion. The research results provided important reference values for efficiently implementing water diversion projects. The main conclusions are as follows:

(1) From the perspective of time variation characteristics, NDVI, temperature, and precipitation showed an upward trend during 2001–2020, indicating that hydrothermal conditions were the main factors influencing vegetation growth.

(2) From the perspective of spatial change characteristics, taking 2013 as the reference year, the NDVI showed a relatively obvious improvement trend overall because of water diversion, and there was spatial heterogeneity. The southwest is in the receiving area, and the change was obvious. The central part remains outside the influence of the water intake area and has not changed. A large range in vegetation was observed in the northeast, and it has shown fluctuating changes in recent years because this region is close to the Yellow River wetland and irrigation area and has relatively sufficient water conditions to maintain a certain level of vegetation coverage.

(3) Based on the above research results, we extracted the Bayin Wenduer Wetland in the southwest water-receiving area and constructed a mechanism set for NDVI. Multiple linear regression, support vector machine, random forest, and deep neural network can reflect the comprehensive effects of various factors on the NDVI. Among them, random forests and deep neural networks have the best simulation effects and can be used to predict the water diversion range under future climate conditions and vegetation growth levels, which is significant for the high-quality operation of water diversion projects.

On the whole, the methods proposed in this paper and the conclusions obtained have high application value and can provide a reference for the research work in similar areas around the world, which has important significance.

Author Contributions: Conceptualization, M.Y. and H.W. (Hao Wang); Data curation, H.W. (Hejia Wang) and L.N.; Formal analysis, L.N.; Funding acquisition, M.Y. and H.W. (Hejia Wang); Investigation, X.Z. and M.Y.; Methodology, L.N. and M.Y.; Project administration, P.M. and H.M.; Resources, P.M., H.M. and H.W. (Hejia Wang); Software, L.N.; Supervision, M.Y. and H.W. (Hejia Wang); Validation, M.Y. and H.W. (Hejia Wang); Visualization, L.N.; Writing—original draft, L.N.; Writing—review and editing, M.Y. and H.W. (Hejia Wang). All authors have read and agreed to the published version of the manuscript.

Funding: This research was funded through the Water Science and Technology Project of Ordos City (No: ESKJ2023-001) and the independent research project of the State Key Laboratory of Watershed Water Cycle Simulation and Regulation: National Water Model Development (Phase I) (No: WR110146B0062024).

Data Availability Statement: The authors do not have permission to share data.

Conflicts of Interest: The authors have no conflicts of interest to declare that are relevant to the content of this article.

Abbreviations

MODIS	moderate-resolution imaging spectroradiometer
NDVI	normalized difference vegetation index
CN05.1	China Meteorological Forcing Dataset 05.1
MOD13A3	MOD13A3 NDVI Monthly 1 km Vegetation Index Data
RF	Random Forest
CART	classification regression tree
SVM	Support vector machine
OA	Overall Accuracy
LUCC	Land Use and Land Cover Change
Pre	precipitation
SSD	sunshine duration
Tem	temperature
RHU	relative humidity

References

1. Wang, W.Z.; Hu, P.; Yang, Z.F.; Wang, J.; Zhao, J.; Zeng, Q.; Liu, H.; Yang, Q. Prediction of NDVI dynamics under different ecological water supplementation scenarios based on a long short-term memory network in the Zhalong Wetland, China. *J. Hydrol.* **2022**, *608*, 127626. [CrossRef]
2. Wang, S.D.; Cui, D.Y.; Wang, L.; Peng, J. Applying deep-learning enhanced fusion methods for improved NDVI reconstruction and long-term vegetation cover study: A case of the Danjiang River Basin. *Ecol. Indic.* **2023**, *155*, 111088. [CrossRef]
3. Zhang, M.; Wang, S.; Fu, B.; Gao, G.; Shen, Q. Ecological effects and potential risks of the water diversion project in the Heihe River Basin. *Sci. Total Environ.* **2018**, *619–620*, 794–803. [CrossRef]
4. Gu, X.L.; Guo, E.L.; Yin, S.; Wang, Y.F.; Wan, Z.Q.; Wang, J. Effects of Yellow River Diversion Project on vegetation in the northern margin of Kubuqi Desert. *Chin. J. Ecol.* **2021**, *40*, 2678–2688. [CrossRef]
5. Liu, Y.; Li, Z.; Chen, Y.; Li, Y.; Li, H.; Xia, Q.; Kayumba, P.M. Evaluation of consistency among three NDVI products applied to High Mountain Asia in 2000–2015. *Remote Sens. Environ.* **2022**, *269*, 112821. [CrossRef]
6. Cano, D.; Cacciuttolo, C.; Custodio, M.; Nosetto, M. Effects of Grassland Afforestation on Water Yield in Basins of Uruguay: A Spatio-Temporal Analysis of Historical Trends Using Remote Sensing and Field Measurements. *Land* **2023**, *12*, 185. [CrossRef]
7. Wang, X.; Geng, X.; Liu, B.; Cai, D.; Li, D.; Xiao, F.; Zhu, B.; Hua, T.; Lu, R.; Liu, F. Desert ecosystems in China: Past, present, and future. *Earth Sci. Rev.* **2022**, *234*, 104206. [CrossRef]
8. Ghebrezgabher, M.G.; Yang, T.; Yang, X.; Sereke, T.E. Assessment of NDVI variations in responses to climate change in the Horn of Africa. *Egypt. J. Remote Sens. Space Sci.* **2020**, *23*, 249–261. [CrossRef]
9. Nan, L.; Yang, M.; Wang, H.; Wang, H.; Dong, N. An innovative correction–fusion approach for multi-satellite precipitation products conditioned by gauge background fields over the Lancang River Basin. *Remote Sens.* **2024**, *16*, 1824. [CrossRef]

10. Zhang, X.; Liu, K.; Li, X.; Wang, S.; Wang, J. Vulnerability assessment and its driving forces in terms of NDVI and GPP over the Loess Plateau, China. *Phys. Chem. Earth* **2022**, *125*, 103106. [CrossRef]
11. Jiang, L.; Liu, Y.; Wu, S.; Yang, C. Analyzing ecological environment change and associated driving factors in China based on NDVI time series data. *Ecol. Indic.* **2021**, *129*, 107933. [CrossRef]
12. He, P.; Xu, L.; Liu, Z.; Jing, Y.; Zhu, W. Dynamics of NDVI and its influencing factors in the Chinese Loess Plateau during 2002–2018. *Reg. Sustain.* **2021**, *2*, 36–46. [CrossRef]
13. Han, J.C.; Huang, Y.; Zhang, H.; Wu, X. Characterization of elevation and land cover dependent trends of NDVI variations in the Hexi region, northwest China. *J. Environ. Manag.* **2019**, *232*, 1037–1048. [CrossRef] [PubMed]
14. Shen, C.; Ma, R. Estimating suitable hydrothermal conditions for vegetation growth for land use cover across China based on maximum-probability-density monthly NDVI. *Remote Sens. Appl. Soc. Environ.* **2023**, *30*, 100958. [CrossRef]
15. Hejduk, L.; Kaznowska, E.; Wasilewicz, M.; Hejduk, A. Dynamics of the Natural Afforestation Process of a Small Lowland Catchment and Its Possible Impact on Runoff Changes. *Sustainability* **2021**, *13*, 10339. [CrossRef]
16. Chen, P.; Wang, S.; Song, S.; Wang, Y.; Wang, Y.; Gao, D.; Li, Z. Ecological restoration intensifies evapotranspiration in the Kubuqi Desert. *Ecol. Eng.* **2022**, *175*, 106504. [CrossRef]
17. Du, H.; Xue, X.; Wang, T. Estimation of saltation emission in the Kubuqi Desert, North China. *Sci. Total Environ.* **2014**, *479–480*, 77–92. [CrossRef]
18. Formica, A.F.; Burnside, R.J.; Dolman, P.M. Rainfall validates MODIS-derived NDVI as an index of spatio-temporal variation in green biomass across non-montane semi-arid and arid Central Asia. *J. Arid Environ.* **2017**, *142*, 11–21. [CrossRef]
19. Gu, J.; Li, X.; Huang, C.; Okin, G.S. A simplified data assimilation method for reconstructing time-series MODIS NDVI data. *Adv. Space Res.* **2009**, *44*, 501–509. [CrossRef]
20. Kumar, B.P.; Babu, K.R.; Anusha, B.N.; Rajasekhar, M. Geo-environmental monitoring and assessment of land degradation and desertification in the semi-arid regions using Landsat 8 OLI/TIRS, LST, and NDVI approach. *Environ. Chall.* **2022**, *8*, 100578. [CrossRef]
21. Beck, H.E.; McVicar, T.R.; van Dijk, A.I.J.M.; Schellekens, J.; de Jeu, R.A.M.; Bruijnzeel, L.A. Global evaluation of four AVHRR–NDVI data sets: Inter comparison and assessment against Landsat imagery. *Remote Sens. Environ.* **2011**, *115*, 2547–2563. [CrossRef]
22. Wang, Z.; Wang, Y.; Liu, Y.; Wang, F.; Deng, W.; Rao, P. Spatiotemporal characteristics and natural forces of grassland NDVI changes in Qilian Mountains from a sub-basin perspective. *Ecol. Indic.* **2023**, *157*, 111186. [CrossRef]
23. Zou, L.; Zhang, Y.; Chen, T.; Liu, H. Evolution characteristics of precipitation and runoff in the Hanjiang River Basin. *J. China Hydrol.* **2023**, *43*, 103–109. [CrossRef]
24. Sun, Z.; Mao, Z.; Yang, L.; Liu, Z.; Han, J.; Wanag, H.; He, W. Impacts of climate change and afforestation on vegetation dynamic in the Mu Us Desert, China. *Ecol. Indic.* **2021**, *129*, 108020. [CrossRef]
25. Mehmood, K.; Anees, S.A.; Rehman, A.; Pan, S.; Tariq, A.; Zubair, M.; Liu, Q.; Rabbi, F.; Khan, K.A.; Luo, M. Exploring spatiotemporal dynamics of NDVI and climate-driven responses in ecosystems: Insights for sustainable management and climate resilience. *Ecol. Inform.* **2024**, *80*, 12532. [CrossRef]
26. Liu, Q.; Liu, L.; Zhang, Y.; Wang, Z.; Wu, J.; Li, L.; Li, S.; Paudel, B. Identification of impact factors for differentiated patterns of NDVI change in the headwater source region of Brahmaputra and Indus, Southwestern Tibetan Plateau. *Ecol. Indic.* **2021**, *125*, 107604. [CrossRef]
27. Yang, T.X.; Yue, C.J. Research on hydrometeor classification of convective weather based on SVM by dual linear polarization radar. *Torrential Rain Disasters* **2019**, *38*, 297–302. [CrossRef]
28. Jin, H.; Chen, X.; Wang, Y.; Zhong, R.; Zhao, T.; Liu, Z.; Tu, X. Spatio-temporal distribution of NDVI and its influencing factors in China. *J. Hydrol.* **2021**, *603*, 127129. [CrossRef]
29. Liang, J.; Chen, C.; Sun, W.; Yang, G.; Liu, Z.; Zhang, Z. Spatiotemporal land use/cover change dynamics in Hangzhou Bay, China, using long-term Landsat time series and GEE platform. *Natl. Remote Sens. Bull.* **2023**, *27*, 1480–1495. [CrossRef]
30. Verhoeven, V.B.; Dedoussi, I.C. Annual satellite-based NDVI-derived land cover of Europe for 2001–2019. *J. Environ. Manag.* **2022**, *302*, 113917. [CrossRef]
31. Chouari, W. Assessment of vegetation cover changes and the contributing factors in the Al-Ahsa Oasis using Normalized Difference Vegetation Index (NDVI). *Reg. Sustain.* **2024**, *5*, 100111. [CrossRef]
32. Wu, X.; Gao, Y.; Dang, X.; Du, B.; Zhang, H.; Bao, X. Temporal and spatial variation of vegetation coverage in Kubuqi Desert from 1989 to 2019. Bull. *Soil Water Conserv.* **2022**, *42*, 300–306. [CrossRef]
33. Jia, Q.; Gao, X.; Jiang, Z.; Li, H.; Guo, J.; Lu, X.; Yonghong Li, F. Sensitivity of temperate vegetation to precipitation is higher in steppes than in deserts and forests. *Ecol. Indic.* **2024**, *166*, 112317. [CrossRef]
34. Zhu, Y.; Zhang, J.; Zhang, Y.; Qin, S.; Shao, Y.; Gao, Y. Responses of vegetation to climatic variations in the desert region of northern China. *CATENA* **2019**, *175*, 27–36. [CrossRef]
35. Yan, J.; Zhang, G.; Ling, H.; Han, F. Comparison of time-integrated NDVI and annual maximum NDVI for assessing grassland dynamics. *Ecol. Indic.* **2022**, *136*, 108611. [CrossRef]
36. Yang, J.; Yan, D.; Yu, Z.; Wu, Z.; Wang, H.; Liu, W.; Liu, S.; Yuan, Z. NDVI variations of different terrestrial ecosystems and their response to major driving factors on two side regions of the Hu-Line. *Ecol. Indic.* **2024**, *2024*, 111667. [CrossRef]

37. Dai, S.P.; Zhang, B.; Wang, Q.; Ma, Z.H.; Zou, Y.; Zhang, Y.N. Variation in grassland vegetation NDVI and its ten-day response to temperature and precipitation in the Qilian Mountains. *Resour. Sci.* **2010**, *32*, 1769–1776.
38. Hossain, M.L.; Li, J. NDVI-based vegetation dynamics and its resistance and resilience to different intensities of climatic events. *Glob. Ecol. Conserv.* **2021**, *30*, e01768. [CrossRef]
39. Fan, X.; Liu, Y. A global study of NDVI difference among moderate-resolution satellite sensors. *ISPRS J. Photogramm.* **2016**, *121*, 177–191. [CrossRef]
40. Faheem, Z.; Kazmi, J.H.; Shaikh, S.; Arshad, S.; Noreena Mohammed, S. Random forest-based analysis of land cover/land use LCLU dynamics associated with meteorological droughts in the desert ecosystem of Pakistan. *Ecol. Indic.* **2024**, *159*, 111670. [CrossRef]
41. Lin, M.; Hou, L.; Qi, Z.; Wan, L. Impacts of climate change and human activities on vegetation NDVI in China's Mu Us Sandy Land during 2000–2019. *Ecol. Indic.* **2022**, *142*, 109164. [CrossRef]
42. Zhao, H.; Zhai, X.; Li, S.; Wang, Y.; Xie, J.; Yan, C. The continuing decrease of sandy desert and sandy land in northern China in the latest 10 years. *Ecol. Indic.* **2023**, *154*, 110699. [CrossRef]
43. Ding, Y.; He, X.; Zhou, Z.; Hu, J.; Cai, H.; Wang, X.; Li, L.; Xu, J.; Shi, H. Response of vegetation to drought and yield monitoring based on NDVI and SIF. *CATENA* **2022**, *219*, 106328. [CrossRef]
44. Zhang, Y.; Jiang, X.; Lei, Y.; Gao, S. The contributions of natural and anthropogenic factors to NDVI variations on the Loess Plateau in China during 2000–2020. *Ecol. Indic.* **2022**, *143*, 109342. [CrossRef]
45. Xu, Y.; Dai, Q.Y.; Zou, B.; Xu, M.; Feng, Y.X. Tracing climatic and human disturbance in diverse vegetation zones in China: Over 20 years of NDVI observations. *Ecol. Indic.* **2023**, *156*, 111170. [CrossRef]
46. Yan, Z.; Li, Z.; Li, P.; Zhao, C.; Xu, Y.; Cui, Z.; Sun, H. Spatial and temporal variation of NDVI and its driving factors based on geographical detector: A case study of GuanZhong plain urban agglomeration. *Remote Sens. Appl. Soc. Environ.* **2023**, *32*, 101030. [CrossRef]
47. Liu, C.; Yan, X.; Jiang, F. Desert vegetation responses to the temporal distribution patterns of precipitation across the northern Xinjiang, China. *CATENA* **2021**, *206*, 105544. [CrossRef]
48. Zhou, Y.G.; Li, H.Y.; Wu, Z.F.; Wang, Z.; Yin, J.; Qing, D.; Hasi, E. Sand fixation mechanism and effect evaluation of sand barriers in Mu Us sandy land, China. *Chin. Sci. Bull.* **2023**, *68*, 1312–1329. (In Chinese) [CrossRef]
49. Li, C.L.; Song, Y.T.; Zhang, J.; Wu, Y.N.; Sun, L. The spatiotemporal pattern and prediction model of NDVI in Qiangtang grassland based on random forest algorithm. *Chin. J. Ecol.* **2024**, *43*, 1664–1673. [CrossRef]
50. Jin, Z.R.; Feng, Q.S.; Wang, R.J.; Liang, T.G. A study of grassland aboveground biomass on the Tibetan Plateau using MODIS data and machine learning. *J. Arid Environ.* **2022**, *31*, 1–17. [CrossRef]
51. Huang, J.W.; Cai, R.H.; Yao, R.; Wang, S.C.; Teng, Z.W. Application of Deep neural network method to discrimination and forecasting of precipitation type. *Meteorol. Mon.* **2021**, *47*, 317–326. [CrossRef]
52. Zhang, Y.Z.; Wu, P.H.; Duan, S.B.; Yang, H.; Yin, Z.X. Downscaling of Landsat 8 land surface temperature products based on Deep neural network. *Natl. Remote Sens. Bull.* **2021**, *25*, 1767–1777. [CrossRef]
53. Li, X.Y.; Zhang, W. Thinking and countermeasures of promoting ecological environmental water management. *Water Resour. Dev. Res.* **2014**, *9*, 44–51. [CrossRef]

Disclaimer/Publisher's Note: The statements, opinions and data contained in all publications are solely those of the individual author(s) and contributor(s) and not of MDPI and/or the editor(s). MDPI and/or the editor(s) disclaim responsibility for any injury to people or property resulting from any ideas, methods, instructions or products referred to in the content.